



Science Arts & Métiers (SAM)

is an open access repository that collects the work of Arts et Métiers Institute of Technology researchers and makes it freely available over the web where possible.

This is an author-deposited version published in: <https://sam.ensam.eu>
Handle ID: <http://hdl.handle.net/10985/6884>

To cite this version :

Baris AYKENT, Damien PAILLOT, Andras KEMENY, Frédéric MERIENNE - A LQR washout algorithm for a driving simulator equipped with a hexapod platform : the relationship of neuromuscular dynamics with the sensed illness rating - In: CONFERE 2012, Italy, 2012-07-05 - CONFERE 2012 - 2012

Any correspondence concerning this service should be sent to the repository

Administrator : scienceouverte@ensam.eu



A LQR WASHOUT ALGORITHM FOR A DRIVING SIMULATOR EQUIPPED WITH A HEXAPOD PLATFORM: THE RELATIONSHIP OF NEUROMUSCULAR DYNAMICS WITH THE SENSED ILLNESS RATING

Baris AYKENT¹, Damien PAILLOT¹, Frédéric MERIENNE¹, Andras KEMENY^{1,2}

¹CNRS LeZi Arts et Métiers ParisTech, 2 Rue T. Dumorey, 71100 Chalon-sur-Saône, France

²Technical Centre for Simulation, RENAULT, Guyancourt, France

ABSTRACT

This study proposes a method and an experimental validation to analyze dynamics response of the drivers with respect to the type of the control used in the hexapod driving simulator. In this article, two different forms of motion platform tracking control have been performed:

- Classical motion cueing algorithm
- LQR motion cueing algorithm

For each situation, the EMG (electromyography) data have been registered from arm muscles of the drivers (flexor carpi radialis, brachioradialis). In addition, the acceleration based illness ratings (IR) have been computed.

In order to process the data of the EMG and IR, the linear regression with a significance level of 0.05 has been assigned. Three cases have been evaluated:

- 1) Time exposure neuromuscular dynamics and vestibular–vehicle level conflict illness ratings
- 2) Time exposure neuromuscular dynamics and vestibular level sensed illness ratings
- 3) Impulse dynamics effect between the neuromuscular (EMG) and the vestibular dynamics (IR)

The results have showed that:

- a) *The vibration exposure condition:* When the total RMS acceleration frequency weighted average IR increases, the EMG average total power increases too by driving the classical motion cueing algorithm. However, in contrast to this, the EMG average RMS total power decreases while the IR increases during the LQR motion cueing algorithm.
- b) *Impulse effect condition:* As the IR augments; the EMG average RMS total power also increases for the optimal motion cueing algorithm but it decreases for the classical algorithm.

Key words: Motion cueing, motion sickness, LQR, optimal control, EMG analysis, dynamic driving simulators

1 INTRODUCTION

Multi-sensory fusion (visual, auditory, haptic, inertial, vestibular, neuromuscular) [Angelaki, 2009] plays important roles to represent a proper sensation (objectively) and so a perception (subjectively as cognition) in driving simulators. For a same scenario, the driver has to react in the same way as in reality in terms of ‘self motion’. To enable this behavior, the driving simulator must enhance the virtual immersion of the subject in the driving situation. The subject has to perceive the motion of his own body in the virtual scene of the virtual car as he will have in a real car. For that reason, restituting the inertial cues on driving simulators is essential to acquire a more proper functioning [Kolanski, 1995]. Simulation sickness has been one of the main research topics for the driving simulators. It was assessed between dynamic and static simulators [Curry, 2002, Watson, 2000]. However, there has been a very few publications of vehicle-vestibular cue conflict based illness rating approach and its correlation with the neuromuscular dynamics for that kind of research. In order to reduce the simulator sickness, the difference between the accelerations through the visual and the vestibular cues have to be

minimized (cost function minimization via linear quadratic regulator which is a certain type of optimal control, in this paper). Because of that fact, this paper addresses the simulator motion sickness as a correlated function of this deviation for the both cues with the EMG RMS total power analysis results for the subjects who have joined in those experiments. Due to the restricted workspace, it is not possible to represent the vehicle dynamics continuously with scale 1 to 1 on the motion platform [Moog FCS, 2006]. Nevertheless, the most desired aim is to minimize the deviation of the sensed accelerations between the represented dynamics as realistic as possible depending on the driving task. This research work has been performed under the dynamic operations of the SAAM driving simulator as with a classical and a LQR controlled tracking of the hexapod platform of the SAAM dynamic driving simulator. It is obvious that inertial restitution addresses a significant role to maintain a developed fidelity of the driver behaviors on diving simulators The dynamic simulators are being used since the mid 1960s (Stewart platform) [Stewart, 1965-1966] firstly for the flight simulators, then the use has spread to the automotive applications. The utilization scope diversifies from driver training to research purposes such as; vehicle dynamics control, advanced driving assistance systems (ADAS), motion and simulator sickness, etc. The dynamic driving simulator SAAM (Simulateur Automobile Arts et Métiers) involves a 6 DOF (degree of freedom) motion system. It acts around a RENAULT Twingo 2 cabin with the original control instruments (gas, brake pedals, steering wheel). The visual system is realized by an approximate 150° cylindrical view. Within the cabin, the multi-level measuring techniques (XSens motion tracker, and Biopac EMG (electromyography) device) [AcqKnowledge® 4, 2011] are available, which have been already used with numerous attempts such as sinus steer test, NATO chicane, etc. The visual accelerations of translations (longitudinal X, lateral Y and vertical Z axes) as well as the visual accelerations of roll and pitch, which correspond to the vehicle dynamics, were taken into account for the control. Then the platform positions, velocities and accelerations were controlled and fed back to minimize the conflict between the vehicle and the platform levels. The research question about this paper explains a comparative study between an open and a closed loop controlled platform in order to determine the relationship between the spent power by the muscles and the IR to maintain the vehicle pursuing a country road scenario. For the evaluation and the validation procedure [Kim,2010,Watson,2000, Reymond, 2001, Kemeny, 2003, Chen, 2007, Pick, 2004, AcqKnowledge® 4, 2011], the scenario driven on the simulator SAAM with a classical motion cueing and a constrained LQR controlled motion cueing to describe the impact of the feedback control. Some results from a case study are illustrated in the scope of this research with real time controls of the platform at a longitudinal velocity of 60 km/h. The results of this study are discussed also statistically to obtain the distribution of the dynamics behavior for a group of the participants.

2 METHODS

Cabin (vehicle) level

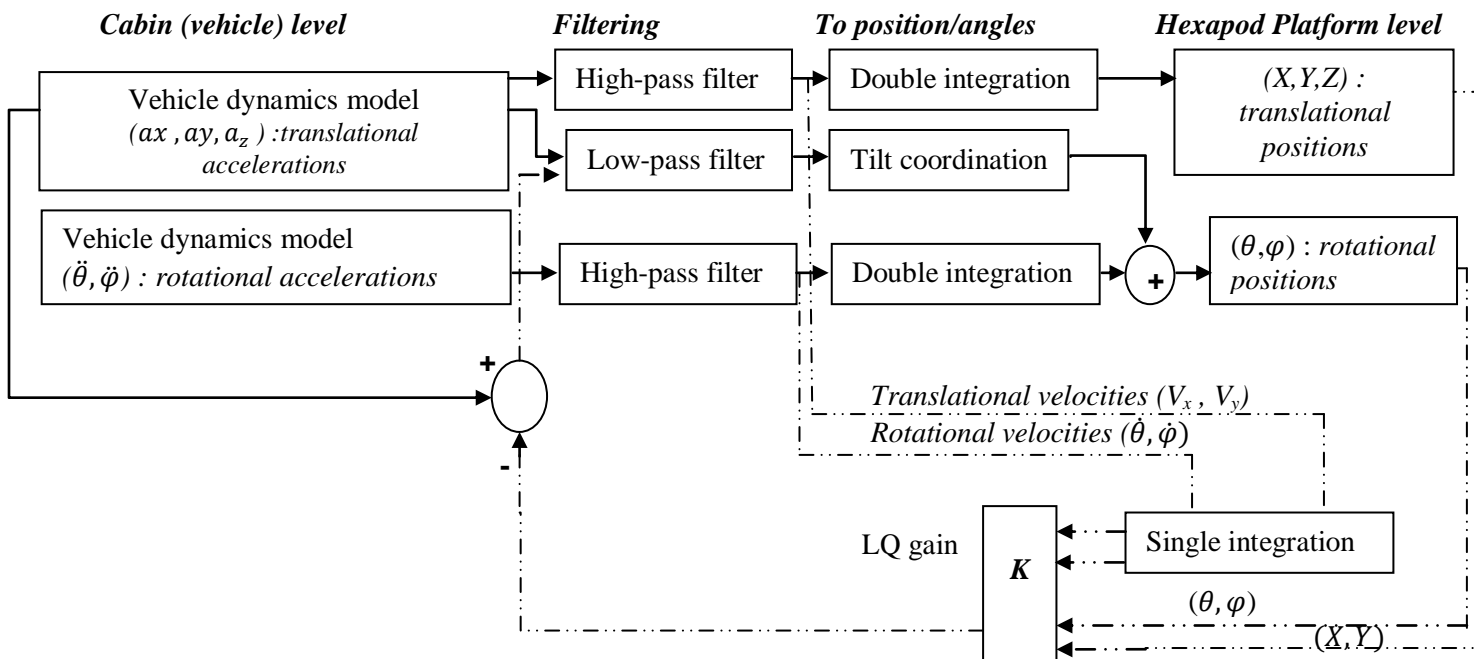


Figure 1. Classical and LQR motion cueing algorithms sketches

The proposed classical motion cueing algorithm's sketch is indicated with continuous lines and arrows where the linear quadratic optimal controlled motion cueing algorithm's sketch has been drawn with discrete lines and arrows (Figure1)

Table 1. Motion cueing algorithm parameters

	Symbol	Classical motion cueing	Longitudinal (gain =1)	Lateral (gain=1)	Roll (gain=0.25)	Pitch (gain=0.25)	Yaw (gain=1)
Hexapod platform (6 DOF)	LP2_mp	6DOF 2nd order LP cut-off frequency			0.3	0.3	
		6DOF 2nd order LP damping			0.7	0.7	
	LP1_mp	6DOF 1st order LP time constant	0.1	0.1			0.1
	HP2_mp	6DOF 2nd order HP cut-off frequency	0.5	0.5			2
		6DOF 2nd order HP damping	1	1			1
	HP1_mp	6DOF 1st order HP time constant	2	2			2

The proposed constrained LQR here uses the same filters, gains (Figure 1 and Table 1) like used in the classical algorithm to compare the effects of the optimal state feedback control of LQR. Linear-quadratic-regulator (LQR) is a modern control engineering technique based on state-space theory for developing optimal dynamic control. LQR design requires a state-space model of the plant. It can focus on the continuous-time case and also on discrete-time LQR design. The discrete time constrained LQR has been referred in this paper. The objective is to regulate the output minimized (platform-vehicle levels' sensed acceleration difference minimization). The plant (dynamic driving simulator) is subject to disturbances and is driven by controls. The LQ regulator consists of an optimal state-feedback gain and a Kalman state estimator. In LQR control, the regulation performance is measured by a quadratic performance criterion. The weighting matrices Q and R are specified via discrete LQR method and define the tradeoff between regulation performance (cost minimization) and control effort (MATLAB Control System's Toolbox User's Guide, 1999, Scokaert, 1998, Ioannou, 1995).

The design step searches a state-feedback law that minimizes the cost function via applying this logic. The minimizing gain matrix is obtained by solving an algebraic *Riccati* equation. This gain is called the linear quadratic optimal gain. Figure 2 illustrates the research method used in this article.

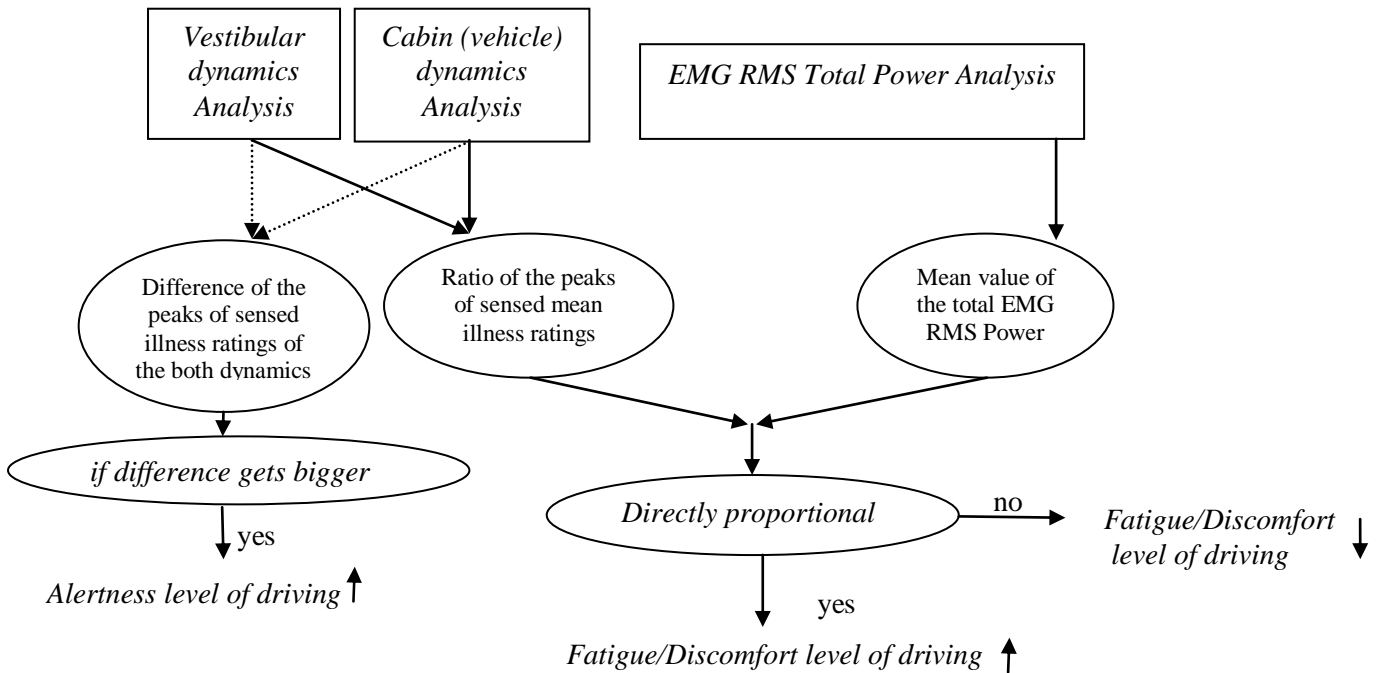


Figure 2. Research method

“K” LQ-gain has been determined by the MATLAB version 7.6.0 ‘dlqr’ code. Then the optimal state feedback motion control algorithm has been integrated with the dynamic driving simulator SAAM with a ‘dll plugin’ which we have been created with Microsoft Visual 2008 C++ used in SCANer studio version 1.1.

Ten healthy participants have attended in the experiments of those three females and seven males with a mean age of 27 ± 4.78 years old and a driving licence holding with a mean experience of 5 ± 4.24 years. Figure 3 shows the trajectory of the country road that we have used in this paper.

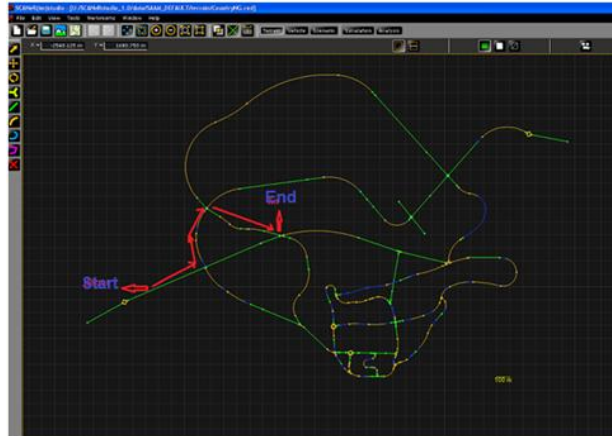


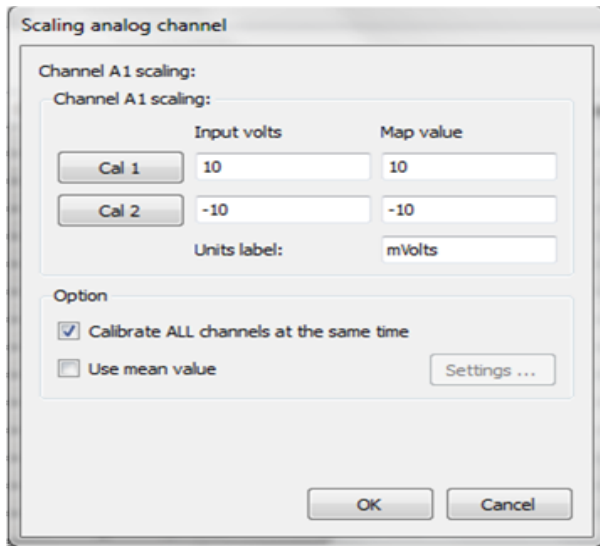
Figure 3. Tested trajectory of a country road

Multi-level data acquisition is performed at three levels as follows:

- **Vehicle level data acquisition (through SCANerStudio software):** Such as the dynamical data of the vehicle model that corresponds to the online simulated vehicle on the simulator in real-time. The used vehicle model is the passenger car defined in the software.
- **Vestibular level data acquisition (through sensor):** Such as the roll, pitch, yaw angles and rates as well as the accelerations in X,Y and Z. The data are calibrated due to three dimensional quaternion orientation. The sampling rate for the data registration during the sensor measurements is 20 Hz. For the calibrated data acquisition, the alignment reset has been chosen which simply combines the object and the heading resets at a single instant in time. This has the advantage that all co-ordinate systems can be aligned with a single action.
- **Electromyography (via Biopac System):** (EMG) is an evaluation method of the electrical activity produced by skeletal muscles. EMG is performed using an instrument called an electromyograph, to realize a record called an electromyogram. An electromyograph detects the electrical potential generated by muscle cells [Mesh electromyography, 2011] when these cells are electrically or neurologically activated. The signals can be analyzed to detect and identify medical abnormalities, muscle activation level, and recruitment order or to analyze the biomechanics of human or animal movements [Mesh electromyography, 2011].

By using the Biopac systems, several frequency and time domain techniques may be used for data reduction of EMG signals [AcqKnowledge® 4, 2011]. For this study, it has been chosen to be concerned to the EMG RMS (root mean square: which is a product of longitudinal, lateral and vertical dynamics related dissipated power) power analysis (V^2/Hz in unit) in time domain, in order to investigate their associations with the acceleration based IR RMS ($m/s^{1.5}$ in unit, which is a product of longitudinal, lateral and vertical acceleration related conflict in dynamics, Eq (1)).

For the calibration of the electromyography, a gain of 1000 has been used. And the Figure 4a and 4c depict the calibration of the analog channels because during the experiments, the electrical activities of the muscles have been registered via two analog channels.



a)

b)



c)

Figure 4. EMG analysis

Electrodes in black circle are connected to flexor carpi radialis muscle where the electrodes in red circle are connected to brachioradialis muscles. We have measured and saved the electrical activity changes on the brachioradialis and flexor carpi radialis muscles. In this paper, we have explained the results which have been taken from the muscle ‘flexor carpi radialis’ (Figures 4b, 4c)

3 RESULTS AND DISCUSSION

According to ISO 2631-1, RMS acceleration values in each axis are defined to more closely reflect the health hazard exposed in the human body. Coefficients are described by ISO 2631-1 on the basis of the frequency and the direction of vibration being exposed to the body. Coefficients of $\omega_k = 0.426$ (cephalocaudal axis) and $\omega_d = 0.067$ (anteroposterior and mediolateral axes) have been used to obtain frequency weighted RMS acceleration in each axe (Eq. (1)). For the evaluation of the health effects $k_x=1.4$, $k_y=1.4$, $k_z=1$ are chosen. We have calculated the IR RMS at both “vehicle” and “vestibular” levels of that we substitute to the “ a_x , a_y and a_z ” for vehicle and vestibular levels respectively (Abercromby, 2007, Griffin, 2004, Benson, 1988, ISO 2631-1, 1997).

$$RMS IR_{total} = \sqrt{(k_x \cdot \omega_k \cdot a_x)^2 + (k_y \cdot \omega_d \cdot a_y)^2 + (k_z \cdot \omega_d \cdot a_z)^2} \quad (1)$$

Figures 5, 6 and 7 explain the impulse dynamics and the total vibration exposition effects in terms of EMG RMS power (V^2/Hz) and IR RMS ($m/s^{1.5}$) relationships. In order to assess the relationships, we have used XLSTAT 2012.

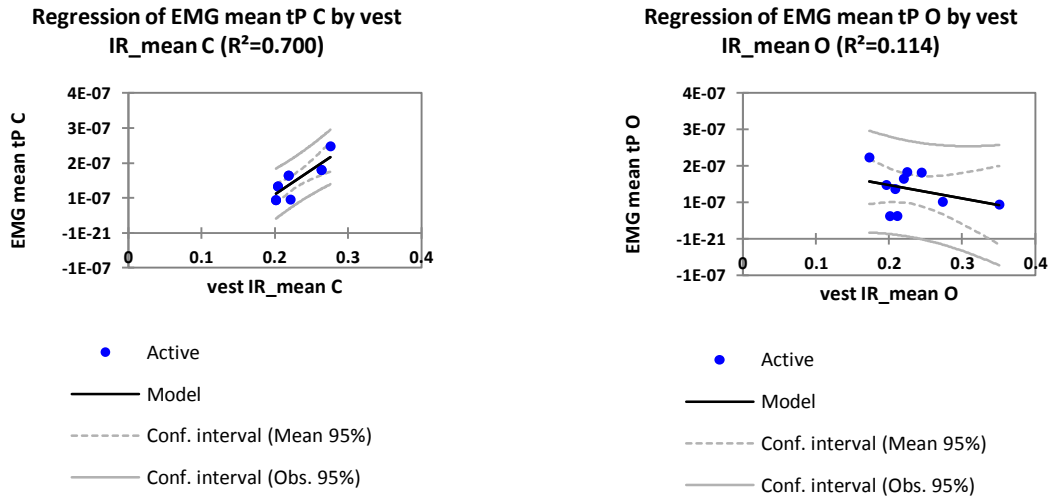


Figure 5. Vestibular illness rating and EMG power analysis relationships

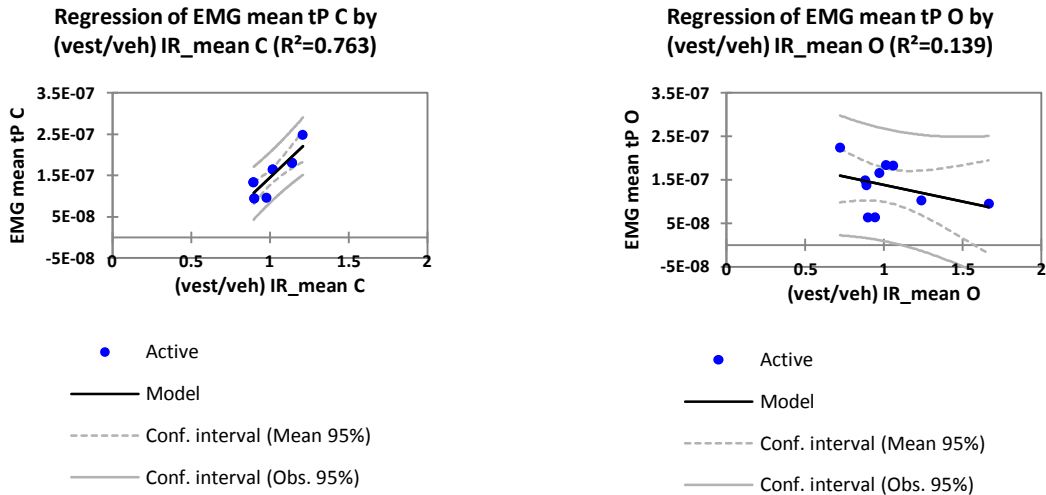


Figure 6. Vestibular to vehicle levels ratio (sensorial conflict) rating and EMG power analysis relationships

C refers to the classical motion cueing algorithm while the O refers to the optimal LQR motion cueing algorithm (Figures 5, 6 and 7).

Figures 5 and 6 are giving the relationships (from the slope of the curves) for the both algorithms of the total scenario, which have lasted approximately 120-145 s differing in the subjects, between the time averaged EMG total power (*EMG mean tP*) and the time averaged IRs (*vest IR_mean*: time averaged vestibular sensed illness rating, *(vest/veh) IR_mean*: time averaged vestibular to vehicle level illness rating ratio) as only at ‘vestibular level’ and as ‘a ratio of vestibular to vehicle levels’ indicating the “conflict”. According to those, it has been proved that by driving the same country road, the power dissipated by the arm muscles fell down (for the LQR optimal motion cueing algorithm compared to classical motion cueing algorithm) by 25.8% and 21.3 % in accordance with considering ‘the vestibular level’ and the ‘vestibular-vehicle level ratios’ respectively for the total time exposure of the scenario for the participants. These results show that; for the classical motion cueing algorithm, during the whole driving phase, the time averaged total power dissipation of the arm muscles are increasing with the increasing level of the both time averaged vestibular and the vestibular to vehicle level ratios illness ratings while the time averaged total power dissipation of the arm muscles are decreasing with the increasing level of the both time averaged vestibular and the vestibular to vehicle level ratios illness ratings for the optimal LQR motion cueing algorithm.

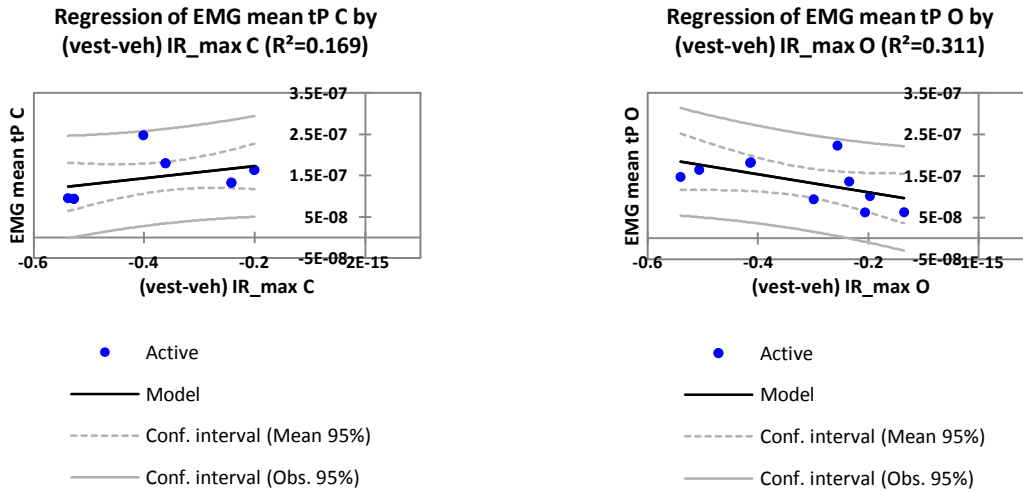


Figure 7. Impulse dynamics effect illness rating and EMG power analysis relationships

Figure 7 shows the relationships (from the slope of the curves) for the both algorithms of the total scenario with respect to the impulse dynamics effect between the time averaged EMG RMS total power ($EMG\ mean\ tP$) and the maximum IR RMS ($(vest-veh)\ IR_max$) as a difference of vestibular to vehicle levels indicating the conflict based on ‘action-reaction’ principle. Because for the whole scenario, the driver’s vestibular organ is dependent to the vehicle and platform levels’ changes in dynamics (Figure 1 and 2). According to this, it has been proved that by driving the same country road; the alertness, in other words the agility level of the drivers (Kaminski, 2011) have increased which let them drive more controllable in the “worst-case situation” (for the LQR optimal motion cueing algorithm compared to the classical motion cueing algorithm) by 47.6 % with respect to the vestibular-vehicle level IR differences for the total time exposure of the scenario for the participants. These results clarify that; for the classical motion cueing algorithm, during the worst case situation (high frequent motion which is an impulse effect dynamics), the time averaged total power dissipation of the arm muscles are decreasing with the increasing level of the time averaged vestibular to vehicle level differences of the illness ratings while the time averaged total power dissipation of the arm muscles are increasing with the increasing level of the time averaged vestibular to vehicle level differences of the illness ratings for the optimal LQR motion cueing algorithm.

4 CONCLUSION AND FUTURE WORKS

It is obvious that if there is a motion, there should be an IR at a certain stage which is a product of accelerations at least one of vehicle-vestibular levels. In this study, we have investigated the vestibular sensed and the vestibular to vehicle ratio (exposure for total scenario) and vestibular-vehicle difference (impulse effect dynamics: high frequent motion) based IRs correlations with the total power spent by the arm muscles.

According to the yielded results of IR in $[m/s^{1.5}]$, the subject ranks his/her illness scores as “0, 1, 2, 3 and greater than 3” given in the following (ISO 2631-1, 1997):

- IR = 0: I felt good
- IR = 1: I felt a mild illness
- IR = 2: felt very bad
- IR \geq 3: I felt absolutely terrible

For all the subjects joined in the experiments, the IRs have been resulted less than 1 (vestibular sensed IRs, Figure 5) which means a comfortable scenario for them, if we only take the illness rating metrics into account.

However, in this article we have offered an extended approach with EMG power analysis. It provides us to conclude up the study more clearly. “Illness rating – EMG mean total power analysis” gives us an idea about the driver’s behaviors as ‘fatigue’ and ‘alertness (agility)’.

Having a closed loop control of the hexapod platform (a LQR optimal motion cueing strategy) has provided a less level of fatigue compared to an open loop control of the hexapod platform (classic motion cueing strategy) with the same filters and gains (Figure 1 and Table 1).

And also, having a closed loop control of the hexapod platform (a LQR optimal motion cueing strategy) has supplied more alertness (agility), that helps the dynamic simulator be driven more controllably, compared to an open loop control of the hexapod platform (a classic motion cueing strategy) with the same filters and gains (Figure 1 and Table 1).

As a conclusion; the LQR optimal motion cueing strategy has optimized the dynamic simulator condition with respect to the classical motion cueing strategy, so that it results as an improved situation for the drivers in terms of the “fatigue” and the “agility (alertness)”.

As prospective work, we would like to evaluate the sickness regarding the roll and pitch velocity perception threshold of the drivers in varied road scenarios, under different controls of the hexapod platform with correlations in inertial, vestibular, neuromuscular cues.

REFERENCES

- Abercromby, A. F. J. et al. (2007), “Vibration Exposure and Biodynamic Responses during Whole-Body Vibration Training”, *Medicine & Science in Sports & Exercise*, pp. 1795-1800.
- AcqKnowledge[®] 4 (2011) Software Guide For Life Science Research Applications, Data Acquisition and Analysis with BIOPAC MP Systems Reference Manual, for AcqKnowledge[®] 4.2 Software & MP150 or MP36R Hardware/Firmware on Windows[®] 7 or Vista or Mac OS[®] X 10.4-10.6, pp.357-358.
- Angelaki D. E., Gu Y. and DeAngelis G. C., (2009) “Multisensory integration: psychophysics, neurophysiology, and computation”, *Current Opinion in Neurobiology*, 19: pp 452-458.
- Aykent, B., Paillot, D., Mérienne, F, Fang, Z., Kemeny, A. (2011) : “Study of the Influence of Different Washout Algorithms on Simulator Sickness for Driving Simulation Task”, *Proceedings of the ASME 2011 World Conference on Innovative Virtual Reality WINVR2011*, Milan, Italy.
- Benson A J: (1988). Motion Sickness. *Medical Aspects of Harsh Environments*, Volume 2, pp 1048-1083, United Kingdom.
- Chen, D., Hart, J., and Vertegaal, R. (2007), “Towards a Physiological Model of User Interruptability”, *IFIP International Federation for Information Processing, INTERACT 2007*, LNCS 4663, Part II, pp. 439 – 451.
- Curry, R.; Artz, B.; Cathey L.; Grant, P. & Greenberg, J. (2002), “Kennedy SSQ results: fixed- vs motion-based FORD simulators”, *Proceedings of Driving Simulation Conference*, pp. 289-300.
- Dichgans, J. & Brandt, T., (1973) . Optokinetic motion sickness and pseudo-coriolis effects induced by moving visual stimuli. *Acta Otolaryngologica*, 76, pp. 339-348.
- DiZio, P., & Lackner, J R., (1988). “The effects of gravito-inertial force level and head movements on post-rotational nystagmus and illusory after-rotation”, *Experimental Brain Research*, Volume 70, Number 3, pp. 485-495, DOI: 10.1007/BF00247597
- DiZio, P., & Lackner, J R., (1989) “Perceived self-motion elicited by postrotary head tilts in a varying gravito-inertial force background”, *Perception & Psychophysics*, Volume 46, Number 2, 114-118, DOI:10.3758/BF03204970
- Griffin, M.J. (1990), “Handbook of Human Vibration”., *Academic Press Limited*, London.
- Griffin, M.J. (2004), “Minimum health and safety requirements for workers exposed to hand-transmitted vibration and whole-body vibration in the European Union; a review”, *Occupational and Environmental Medicine*, pp. 387-397.
- Guedry, F. E., Jr. (1995), “Visual control of habituation to complex vestibular stimulation in man”, Bureau of Medicine and Surgery, *Project MR005.13-6001*, Subtask 1 Report No. 95, NASA Order No. R-93, p. 1-16, U. S. Naval School of Aviation Medicine, U. S. Naval Aviation Medical Center, Pensacola Florida.
- Guedry, F. E. and Montague, E. K., (1961). Quantitative evaluation of the vestibular Coriolis reaction. *Aviation, Space, and Environmental Medicine*, 32(6), pp. 487-500.
- Hall J., R. (1989), “The need for platform motion in modern piloted flight training simulators”, *Tech Mem, FM 35*.
- Ioannou, P.A and Sun, J. (1995), ‘Robust adaptive control’. *Prentice-Hall Inc*.
- ISO 2631-1:1997, (1997) “Mechanical vibration and shock -- Evaluation of human exposure to whole-body vibration -- Part 1: General requirements”. Geneva, Switzerland.

- Kaminski, T. et al. (2011), "ADVANCED CAR DRIVING SIMULATOR – AS 1200-6", *Journal of KONES Powertrain and Transport*, Vol. 18, No. 4.
- Kemeny A. and Panerai, F. (2003), "Evaluating perception in driving simulation experiments", *TRENDS in Cognitive Sciences*, Vol. 7 No. 1, pp 31-37.
- Kennedy, R. S., Berbaum, K. S., Lilienthal, M. G., Dunlap, W. P., Mulligan, B. E., & Funaro, J. F., (1987). Guidelines for alleviation of simulator sickness symptomatology (*Final Report No. NAVTRASYSCEN TR-87-007*). Orlando, FL: Naval Training Systems Center.
- Kim M.S. et al (2010), "Partial range scaling method based washout algorithm for a vehicle driving simulator and its evaluation", *International Journal of Automotive Technology*, Vol. 11, No. 2, pp. 269–275.
- Kolasinski E., M. (1995) 'Simulator Sickness in Virtual Environments', *Army Project Number 2O262785A79I*, Education and Training Technology.
- MATLAB Control Systems Toolbox User's Guide (1999), *version 4.2*.
- MESH ELECTROMYOGRAPHY (2011), *NATIONAL LIBRARY OF MEDICINE - MEDICAL SUBJECT HEADINGS*, MESH, ([HTTP://WWW.NLM.NIH.GOV/CGI/MESH/2011/](http://www.nlm.nih.gov/cgi/mesh/2011/)), REACHED ON 13TH MARCH 2012.
- MOOG FCS, 6 DOF Motion System, (2006) "Motion Drive Algorithm (MDA) Software Tuning Manual Version 1.0", *Document No: LSF-0468*, Revision: A.
- Nehaoua L, Arioui H., Espié S. and Mohellebi, H. (2006), "Motion Cueing Algorithms for Small Driving Simulator", *IEEE International Conference in Robotics and Automation (ICRA06)*, Orlando, Florida.
- Persson R. (2007), "Motion sickness in tilting trains: Description and analysis of the present knowledge", *Literature Study*, ISBN 978-91-7178-680-3.
- Pick, A., J. (2004), "Neuromuscular Dynamics and the Vehicle Steering Task", *PhD thesis*, St Catharine's College, Cambridge University Engineering Department.
- Reason J & Brand J: (1975). "Motion sickness". London: *Academic press*. London.
- Reymond, G., Kemeny, A., Droulez, J., Berthoz A (2001) "Role of lateral acceleration in driving: experiments on a real vehicle and a driving simulator", *Human Factors* 43(3): pp. 483-495.
- Siegler, I., Reymond, G., Kemeny, A. & Berthoz, A. (2001), "Sensorimotor integration in a driving simulator: contributions of motion cueing in elementary driving tasks", *Proceedings of Driving Simulation Conference*, pp 21-32.
- Stewart D., "A platform with six degrees of freedom (1965-1966)," *Proc. Inst. Mech. Eng.*, Vol.180, part I (15), pp.371-386.
- Scokaert, P.O. M, and Rawlings, J.B. (1998), "Constrained Linear Quadratic Regulation", *IEEE TRANSACTIONS ON AUTOMATIC CONTROL*, VOL. 43, NO. 8.
- Watson, G., S. (2000), "A synthesis of simulator sickness studies conducted in a high fidelity driving simulator", *Proceedings of Driving Simulation Conference*, pp. 69-78.